PERGAMON

International Journal of Multiphase Flow 28 (2002) 1617–1629

International Journal of Multiphase Flow

www.elsevier.com/locate/ijmulflow

# Effect of pipe diameter on the drop size in a horizontal annular gas–liquid flow

A. Al-Sarkhi [a], T.J. Hanratty [b,*]

[a] *Department of Mechanical Engineering, Hashemite University, Zarqa 13115, Jordan*
[b] *Department of Chemical Engineering, University of Illinois at Urbana-Champaign, Urbana, IL 61801, USA*

Received 11 September 2001; received in revised form 13 June 2002

**Abstract**

Measurements of the drop size distributions were obtained for air and water flowing in an annular pattern in a 2.54 cm horizontal pipe. A laser diffraction technique was used. The data were obtained at the centerline. These are compared with measurements obtained previously for annular flow of air and water in a horizontal 9.53 cm pipe in the same flow loop and with the same instrumentation. The volume median drop diameter for these two flows was found to increase with pipe diameter and to vary with $D^{0.5}$ for superficial gas velocities larger than 30 m/s.


*Keywords:* Drop size distribution; Annular gas–liquid flow; Laser diffraction

## 1. Introduction

An annular pattern can exist when gas and liquid flow at a high velocity in a pipe. Part of the liquid flows along the wall and part, as drops entrained in the gas. There is an exchange of liquid between the wall and the gas core, whereby drops deposit at the wall and are formed by atomization of the wall film. Under equilibrium conditions the rate of atomization, $R_A$, equals the rate of deposition, $R_D$. A critical parameter needed to understand the behavior of an annular flow is the fraction of the liquid entrained as drops, $E$, which is related to $R_A$ and $R_D$.

A central problem in analyzing annular flows is the prediction of drop size. The rate of deposition is usually defined in terms of a deposition constant, $K_D$,

* Corresponding author. Tel.: +1-217-333-1318; fax: +1-217-333-5052.
*E-mail address:* hanratty@scs.uiuc.edu (T.J. Hanratty).

0301-9322/02/$ - see front matter 
PII: S0301-9322(02)00048-4

$$R_D = K_D C_W \tag{1}$$

where $C_W$ is the concentration at the wall. For vertical flows $C_W$ equals the bulk concentration of drops and, for most cases, $K_D$ is related to the root-mean-square of the velocity fluctuations of the drops. The ratio of the drop turbulence to the fluid turbulence decreases with increasing drop diameter because of the increase in the inertial time constant of the drops.

The influence of drop size in horizontal annular flows is more complicated. Rates of deposition are changed because gravitational settling causes an asymmetric distribution of drops and contributes directly to the local rate of deposition. The influence of gravity on deposition and on the asymmetric distribution of drops increases with increasing drop size.

The focus of this paper is to examine the effect of pipe diameter on drop size in horizontal annular flows. Such information is critically important in predicting the behavior of large diameter pipes.

The theoretical analysis by Tatterson et al. (1977) suggests that

$$\left(\frac{\rho_G U_G^2 \lambda}{\sigma_{st}}\right)^{0.5} \left(\frac{d_p}{\lambda}\right)^{0.5} = \text{constant} \tag{2}$$

where $\lambda$ is the wavelength of the waves on the liquid film which break up to form drops, $\rho_G$ is the gas density, $\sigma_{st}$ is the surface tension, and $U_G$ is the gas velocity. These authors assumed that $\lambda$ varies directly with the film height, $m$, and suggested that $m$ is proportional to the pipe diameter, $D$. The speculations of Tatterson et al., therefore, suggest that

$$d_p \sim D^{0.5} \tag{3}$$

where $d_p$ is the drop diameter and $D$ is the pipe diameter.

The most widely used method to predict drop size is the following empirical correlation developed by Azzopardi (1985) from a consideration of experimental data, mainly for flows in vertical pipes:

$$d_{32} = \lambda_A \left[15.4\left(\frac{\rho_l U_G^2 \lambda_A}{\sigma_{st}}\right)^{-0.58} + 3.5\left(\frac{G_{LE}}{\rho_L U_G}\right)\right] \tag{4}$$

where $d_{32}$ is the Sauter-mean diameter, $\rho_L$ is the liquid density, $G_{LE}$ is the mass flux of entrained drops, and $\lambda_A$ is a Taylor length scale.

$$\lambda_A = \left(\frac{\sigma_{st}}{\rho_L g}\right)^{0.5} \tag{5}$$

Pan and Hanratty (2002) have also used Eq. (4) with $\rho_G$ replacing $\rho_L$ in the first term on the right side and with the constants being replaced by 0.33 and 3.5. There is clearly a difference between Eq. (4) and the measurements reported in this paper in that the drop size is predicted to be independent of pipe diameter.

Reviews of studies of drop size in annular flow are summarized by Azzopardi (1983, 1985, 1997) and Simmons and Hanratty (2001), who present an extensive account of measurements with a Malvern Spraytec R5008 for air and water flowing in a horizontal 9.53 cm pipeline. The present paper presents the results of a study for air and water flowing in a 2.54 cm pipeline. The flow system and the measuring techniques are the same as used by Simmons and Hanratty (2001).

## 2. Description of the experiments

### 2.1. Flow loop

The pipeline used in the experiments was constructed from sections of clear acrylic plastic, whose ends were machined to ensure smooth transitions. A description of the air–water mixing section and of the design of the flow loop can be found in a paper by Al-Sarkhi and Hanratty (2001). Drop size measurements at the centerline of the pipe were made 13 m (500 pipe diameters) from the inlet.

### 2.2. Measurement of drop size

Fig. 1 presents a schematic drawing of the test section and the Malvern RT5008 sizer. A He–Ne laser illuminated the flow field. Light scattered by the drops at small angles is mainly caused by diffraction and the magnitude of the angle varies inversely with the drop size.

The scattered light is analyzed by a set of concentric annular detectors (as shown in Fig. 1) placed at the focal point of a Fourier lens, which converts the incoming rays of scattered light into a far-field diffraction pattern. In this way, the detector picks up light scattered at different angles that are dependent on the drop size and not on the position of the drops in the pipe. A size distribution that has 15 adjustable parameters is assumed. This is used to calculate an energy distribution of the scattered light. The values of the parameters describing the size distribution are adjusted until a best fit between the calculated and measured energy distribution is achieved. The software for the Malvern instrument includes a patented correction for the effect of multiple scattering that allows measurements to be made when only 5% of the incident light beam is transmitted. The instrument used in this study was equipped with a 450 mm lens, which is claimed to give accurate measurements of size distributions with volume median diameters in the range of 2.25–850 μm. Results were obtained for a range of drop concentrations such that the transmission was 30% or greater.

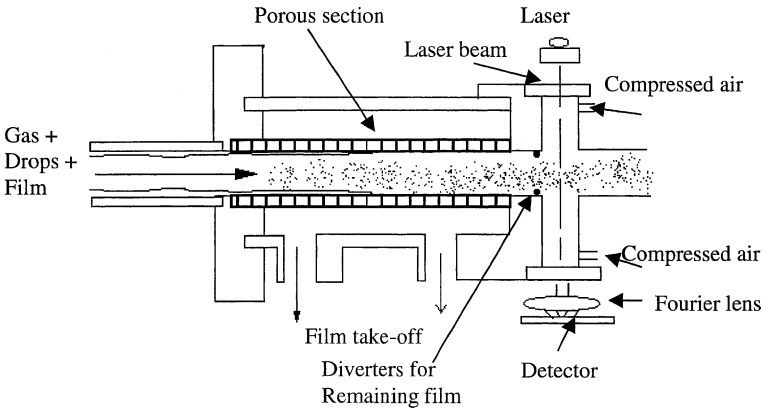


Fig. 1. Sketch of the test section for the removal of the liquid film and of the setup for the Malvern analyzer.

In order for the laser beam to have an unobstructed view of the drops, the liquid film was removed from the wall by using the porous test section shown in Fig. 1 and described by Azzopardi et al. (1996), Hay et al. (1996) and Simmons and Hanratty (2001). The film is forced through the porous wall by the pressure difference between the flow stream and the annular section surrounding the porous wall. The droplets move at a much higher velocity than the film, so their large inertia prevents removal from the flow. The porous wall was installed just before the test section so as to prevent a reforming of the film by drop deposition. Any remaining wall film was detoured around the openings used for the laser beam, by diverters that were attached to the inside of the pipe (see Simmons and Hanratty, 2001). Several experiments have been done on the extension length of the diverter inside the pipe and the position of the diverter before the opening to ensure that no drops are generated by the diverter.

The laser beam was passed through anti-reflectant glass windows. The contamination of these windows by drop impaction was minimized by placing them at a distance from the flow. An air purge system was installed to blow air over the internal surface of the windows. The number of drops that may enter the arm and hit the windows was kept small by maintaining a slight positive pressure in the windows section. Several preliminary studies showed that the drop size distributions were not influenced by the purge air, by the rate of removal of the film or by the diverters.

## 3. Results

### 3.1. Distribution of drop sizes

The distributions obtained with the Malvern instrument were averaged over at least 200 s, so as to give sample sizes with billions of drops.

Fraction volume distributions obtained for superficial gas velocities, $U_{SG}$, of 30–50 m/s are given in Fig. 2 for a superficial liquid velocity of, $U_{SL}$, of 0.041 m/s and in Fig. 3 for $U_{SL} = 0.083$ m/s. The Sauter mean diameter, $d_{32}$, and the volume median diameter, $d_{50}$, representing the measurements are listed in Table 1. The drop diameter below which 10% and 50% of the liquid volume were contained are designated by $d_{10}$ and $d_{50}$ in Table 1. The percent of the light transmitted, $T$, and the concentration of drops, which this suggests, $C_v$, are also listed in Table 1. This could give results on entrainment but the accuracy of this measurement has not been tested.

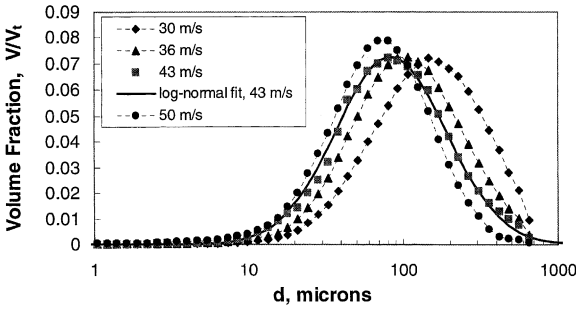


Fig. 2. Volume distribution at $U_{SL} = 0.041$.

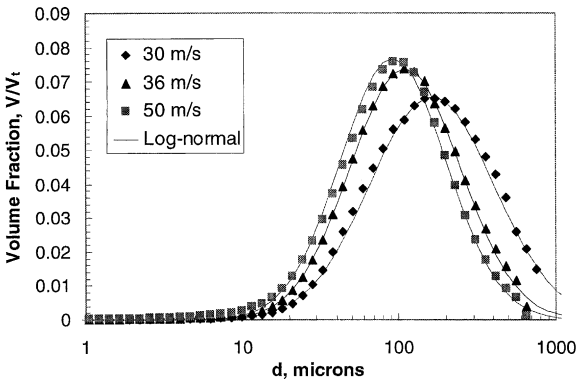


Fig. 3. Volume distribution function at $U_{SL} = 0.083$ m/s.

Table 1
Parameters characterizing the drop size distribution

| Flow matrix | | Malvern parameters | | Experimental parameter | | | | Log-normal parameters | | |
|---|---|---|---|---|---|---|---|---|---|---|
| $U_{SG}$ (m/s) | $U_{SL}$ (m/s) | Obs$(1-T)$ (%) | $C_V$ (ppm) | $d_{32}$ (μm) | $d_{10}$ (μm) | $d_{50}$ (μm) | $d_{90}$ (μm) | $d_{32}$ (μm) | $d_{50}$ (μm) | $\sigma$ |
| 30 | 0.041 | 8.36 | 127.1 | 88.64 | 46.77 | 143.5 | 379.4 | 103 | 145 | 0.82 |
| 30 | 0.05 | 11.49 | 183.1 | 91.33 | 47.64 | 147.2 | 390.4 | 104.5 | 148 | 0.83 |
| 30 | 0.062 | 15.46 | 249.4 | 92 | 47.8 | 147.9 | 397.0 | 106.4 | 156 | 0.87 |
| 30 | 0.083 | 24.29 | 432.1 | 94.66 | 48.4 | 157.6 | 424.09 | 107.3 | 162.3 | 0.92 |
| 30 | 0.104 | 31.98 | 621.7 | 98.25 | 49.88 | 163.62 | 435.13 | 112.9 | 172 | 0.93 |
| 36 | 0.041 | 13.2 | 151.2 | 65.11 | 35.89 | 103.0 | 289.6 | 74.7 | 104.5 | 0.82 |
| 36 | 0.05 | 24.5 | 300.9 | 65.77 | 35.9 | 102.5 | 289.8 | 75.7 | 106.5 | 0.82 |
| 36 | 0.062 | 28.55 | 366.7 | 66.53 | 36.44 | 104.08 | 292.19 | 77.3 | 107.7 | 0.815 |
| 36 | 0.083 | 38 | 542.9 | 69.4 | 37.92 | 108.1 | 299.3 | 79.2 | 109.9 | 0.81 |
| 36 | 0.104 | 47.57 | 762.3 | 71.99 | 39.34 | 112.5 | 311.35 | 84.6 | 115.5 | 0.79 |
| 36 | 0.125 | 53.5 | 946.9 | 78.5 | 41.7 | 121.4 | 316.5 | 88.2 | 121.5 | 0.8 |
| 43 | 0.041 | 25.4 | 275 | 57.3 | 31.07 | 82.76 | 235.3 | 59.4 | 83.1 | 0.82 |
| 43 | 0.05 | 36.16 | 433 | 58.94 | 31.77 | 87.72 | 257.96 | 64.3 | 90.0 | 0.82 |
| 43 | 0.062 | 41.1 | 496.4 | 57.35 | 31.5 | 87.26 | 235.86 | 66.4 | 90.1 | 0.78 |
| 43 | 0.083 | 50.3 | 675.5 | 59 | 33.56 | 94.76 | 252.2 | 70 | 94.6 | 0.77 |
| 43 | 0.104 | 57.82 | 903 | 63.8 | 36.3 | 105.4 | 286.9 | 75.9 | 104.5 | 0.8 |
| 50 | 0.041 | 32.9 | 283 | 43.47 | 25.14 | 71.11 | 183.38 | 54.5 | 72.2 | 0.75 |
| 50 | 0.05 | 43.2 | 421.5 | 45.64 | 26.56 | 75.68 | 193.03 | 56.9 | 75.2 | 0.745 |
| 50 | 0.062 | 50.2 | 552.7 | 48.5 | 28.13 | 81.13 | 208.7 | 61.9 | 81.4 | 0.74 |
| 50 | 0.083 | 59.25 | 802.2 | 54.6 | 31.3 | 93.11 | 248.9 | 67.7 | 91.8 | 0.78 |
| 50 | 0.104 | 65.2 | 1042.2 | 60.34 | 34.05 | 105.23 | 287.2 | 76.2 | 106.7 | 0.82 |
| 50 | 0.125 | 70.5 | 1374.9 | 68.68 | 37.8 | 123.17 | 337.9 | 85.3 | 121.5 | 0.84 |

The curves in Figs. 2 and 3 represent a log-normal distribution,

$$dv = \frac{1}{\sigma\sqrt{2\pi}} \exp\left[ -\frac{1}{2}\left( \frac{\ln d_p - \ln d_{v50}}{\sigma} \right)^2 \right] \frac{dd_p}{d_p} \tag{6}$$

where $dv$ is the fraction of the liquid volume contained in drops with diameters between $dd_p$ and $d_p + dd_p$ and $\sigma$ is the standard deviation. For a log-normal distribution, the Sauter mean diameter, $d_{32}$, is related to the volume median diameter, $d_{50}$, by

$$d_{32} = \frac{d_{50}}{\exp(\sigma^2/2)} \tag{7}$$

The cumulative volume distributions calculated from Eq. (7) plot as straight lines on log-normal paper (log-probability plot). This is illustrated in Figs. 4 and 5 where the drop diameter is normalized with the volume median diameter. (Thus $d/d_{50} = 1.0$ corresponds to a cumulative volume fraction of 50%.) The log-normal parameters $d_{50}$ and $\sigma$ were obtained from straight line fits, such as shown in Figs. 4 and 5 for $U_{SG} = 36$ m/s and for $U_{SG} = 43$ m/s. The Sauter mean diameter was calculated from Eq. (7). These parameters are listed in Table 1. It is noted that the volume median diameter obtained from the log-normal fit and the measured $d_{50}$ are very close. As seen from Figs. 4 and 5, the distributions are approximately similar. However, small effects of liquid flow are noted for very small drop diameters which contain about 2.5% of the drop volume.

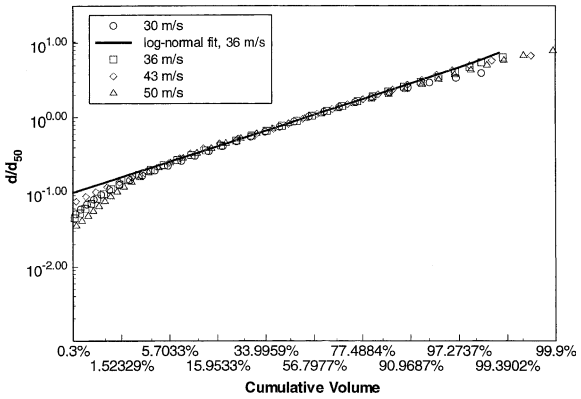


Fig. 4. Log-probability plot for log-normal distribution at $U_{SL} = 0.041$ m/s.

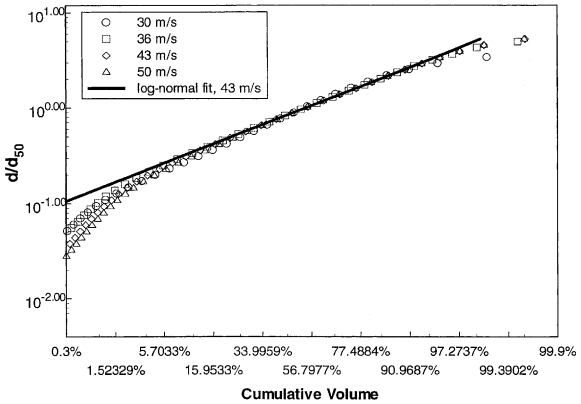


Fig. 5. Log-probability plot for log-normal distribution at $U_{SL} = 0.104$ m/s.

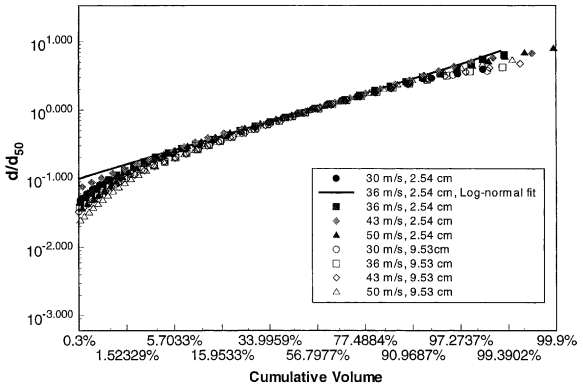


Fig. 6. Log-probability plot at $U_{SL} = 0.041$ m/s of results from the current study and from Simmons and Hanratty (2001).

The results in Figs. 2–4 show that log-normal distributions provide a good fits to the data, except for very small and very large drops (about 2% of the volume).

Fig. 6 presents measurements in a 9.53 cm pipe made below the centerline. The straight line represent a log-normal distribution characterized by $\sigma = 0.82$. A rough agreement with measurements made in a 2.54 cm pipe (also presented in this figure) is noted. However, the departure from a log-normal distribution at small and large drop sizes is more severe in the larger pipe.

### 3.2. Effect of pipe diameter

An examination of the effects of pipe diameter is possible by comparing the results presented in this paper for a pipe with a diameter of 2.54 cm and the results obtained by Simmons and Hanratty (2001) in a 9.53 cm pipe. The measurements in the 2.54 cm pipe were obtained at the centerline. Results were obtained in the 9.53 cm pipe at the centerline, 1.9 cm above the centerline and 1.9 cm below the centerline. A comparison was, therefore, made complicated because effects of liquid flow and of location in the pipe need to be taken into account. The influence of gravity on the spatial distribution of drops should depend, to first order, on the distance from the bottom wall. We, therefore, feel that the results are best compared by considering the data for the 9.53 cm pipe at the position below the centerline. This is done in Fig. 7 where volume median diameters are plotted against the superficial liquid velocity.

The volume median diameter is seen to increase with increasing pipe diameter. This qualitative effect is also seen in Fig. 8 where data at the centerline of the 9.53 cm pipe are used. However, it is to be noted that the $d_{50}$ for the 9.53 cm pipe show slightly different effects of $U_{SL}$ at the centerline and below the centerline. Fig. 9 gives the ratio of the $d_{50}$ obtained in the 9.53 cm pipe and in the 2.54 cm pipe. The squares used results from the 9.53 cm pipe obtained below the centerline; the diamonds are for results obtained at the centerline. Every point was taken at the same superficial gas and liquid velocities. The first three points for different gas velocities were obtained at $U_{SL} = 0.041$ m/s, the second, at 0.053 m/s and the third, at 0.061 m/s. At $U_{SG} = 36$, 43, 50 m/s, $d_{50}$ is seen to vary approximately as the pipe diameter to the 0.5 power. This is, particularly, the case when the data in the 2.54 cm pipe are compared with data in the 9.53 cm pipe obtained below the

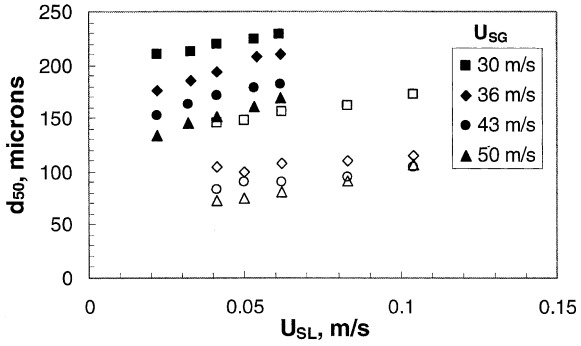


Fig. 7. Comparison of volume median diameters obtained in the 2.54 cm pipeline (open symbols) and in the 9.53 cm pipeline (filled symbols). The data for the 9.53 cm were obtained 1.9 cm below the centerline.

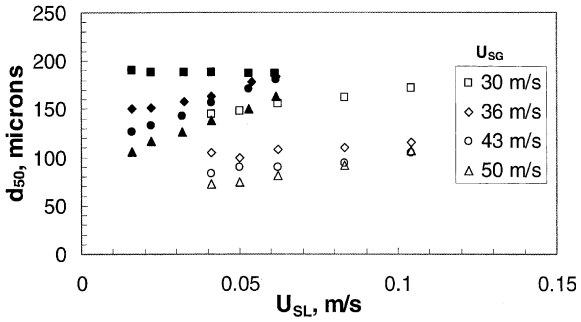


Fig. 8. Comparison of volume median diameters obtained in the 2.54 cm pipeline (open symbols) and in the 9.53 cm pipeline (filled symbols). The data for the 9.53 cm were obtained at the centerline.

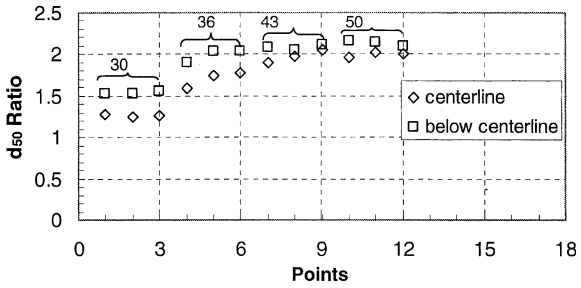


Fig. 9. Ratio of the $d_{50}$ measured in the 9.53 and 2.54 cm pipes. Groups of points for $U_{SL} = 0.041$, 0.053 and 0.061 m/s are presented for $U_{SG} = 30$, 36, 43, and 50 m/s. The diamonds are for points taken at the centerline and the squares, for points below the centerline of the 9.53 cm pipe.

centerline. The data taken at $U_{SG} = 30$ m/s show a smaller effect of pipe diameter than is observed at larger gas velocities. As suggested by Azzopardi (1983, 1985), the mechanism of atomization could be different at low gas velocities. This is particularly, in evidence, by the very large increase in $d_{50}$ observed with a change of gas velocity from 36 to 30 m/s in the 2.54 cm pipe.

### 3.3. Effect of gas velocity

Measurements at different liquid flows were averaged for different gas velocities. These are plotted in Fig. 10. The data for the 9.53 cm pipe at the lowest superficial liquid velocity indicate $d_{50} \sim U_{SG}^{-1.1}$. The data for the 2.54 cm pipe at the lowest superficial liquid velocity give $d_{50} \sim U_{SG}^{-1.16}$. For $U_{SG}$ greater than 30 m/s, $d_{50} \sim U_{SG}^{-1.11}$ if all of the data in Fig. 10 are considered.

Measurements of the Sauter mean, $d_{32}$, diameter and the volume median, $d_{50}$, diameter are presented in Fig. 11 for $U_{SL} = 0.062$ m/s. The filled points were obtained from a log-normal fit and the unfilled points from the data. The $d_{32}$ are smaller than the $d_{50}$ and, therefore, more susceptible to differences in the data at low gas velocities. Therefore, the log-normal fit produces larger $d_{32}$ than a direct analyses of the data. The influence of gas velocity is similar to what is observed for $d_{50}$ in Fig. 8.

A comparison of $d_{32}$ obtained in this study, with the experiments of Simmons and Hanratty (2001) below the centerline of a 9.53 cm pipe and by Ribeiro et al. (1995) in a 3.2 cm pipe is given in Fig. 12 for $U_{SL} = 0.041$ m/s. The data suggest, on average, that $d_{32} \sim U_{SG}^{-1.1}$.

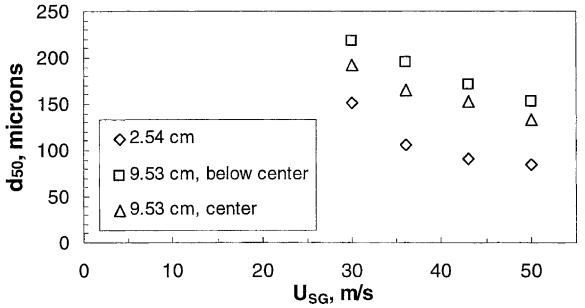


Fig. 10. Effect of $U_{SG}$ on $d_{50}$ for different pipe diameters. The data points represent an average of all the $U_{SL}$ that were studied.

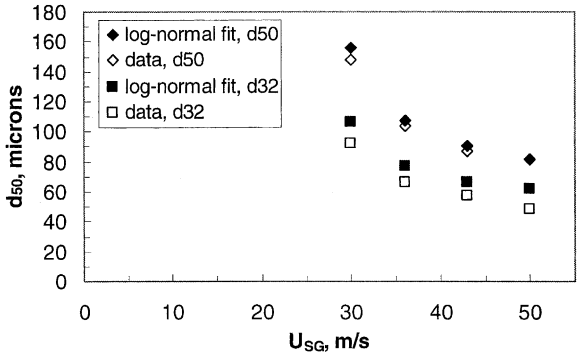


Fig. 11. Effect of superficial gas velocity on $d_{50}$ and $d_{32}$ at $U_{SL} = 0.062$ m/s.

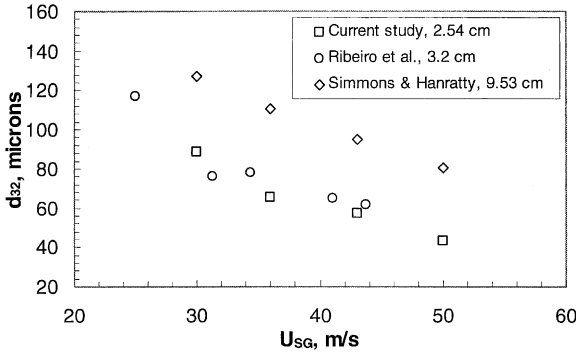


Fig. 12. Comparison of $d_{32}$ at $U_{SL} = 0.041$ m/s. The data of Simmons and Hanratty were obtained below the centerline.

### 3.4. Effect of liquid flow

The effect of liquid flow rate is not simple, nor is it clearly understood, as can be seen in the results presented in Figs. 7 and 8. We have tried to interpret it in terms of the ratio $U_{SL}/U_{SG}$, the fraction of the liquid flowing as a wall film and the liquid flowing as entrained drops. No definite conclusion has been reached. Therefore, the presentation makes a comparison with the approach taken in Eq. (4). This assumes that the drop diameter varies linearly with the volume fraction of entrained drops, $G_{LE}/\rho_L U_G$. Simmons and Hanratty suggested that the results for a 9.53 cm pipe can be correlated as

$$d_{32}U_G^{1.1} = 4.848\frac{G_{LE}}{\rho_L U_G} + 0.0038 \tag{8}$$

An equation of this form that takes account of the effect of pipe diameter and that is a modified version of Eq. (4) is as follows:

$$\left(\frac{d_{32}U_{SG}^2\rho_G}{\sigma}\right)^{0.55}\left(\frac{d_{32}}{D}\right)^{0.45} = 29.5\frac{G_{LE}}{\rho_L U_{SG}} + 0.072 \tag{9}$$

Eq. (9) is plotted in Fig. 13, using data obtained at the centerline of a 2.54 cm pipe, below the centerline of a 9.53 cm pipe and at the centerline of a 9.53 cm pipe. The data of Dallman (1978) and the data of Williams (1990) were used to obtain the fraction of the liquid entrained in the 2.54 cm and the 9.53 cm pipes. The data points obtained at $U_{SG} = 30$ m/e in the 2.54 cm pipe and the data obtained at the centerline in a 9.53 cm pipe were not used in selecting the constants in Eq. (9). A similar correlation for $d_{50}$ is

$$\left(\frac{d_{50}U_{SG}^2\rho_G}{\sigma}\right)^{0.55}\left(\frac{d_{50}}{D}\right)^{0.45} = 51.7\frac{G_{LE}}{\rho_L U_{SG}} + 0.122 \tag{10}$$

### 3.5. Simplified correlation

Eqs. (9) and (10) are difficult to use because data on entrainment are needed. Therefore, the following approximate representations were developed, that ignore the effect of liquid flow and that use results presented earlier in this section:

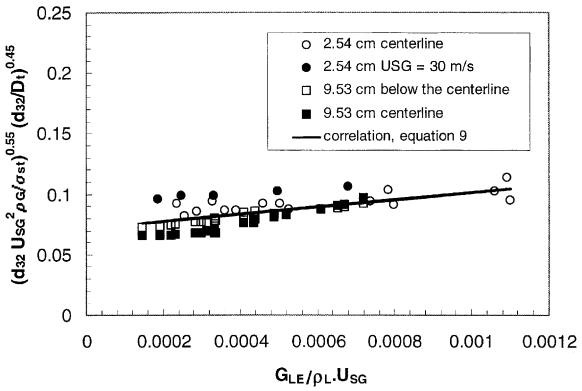


Fig. 13. Comparison of data with Eq. (9).

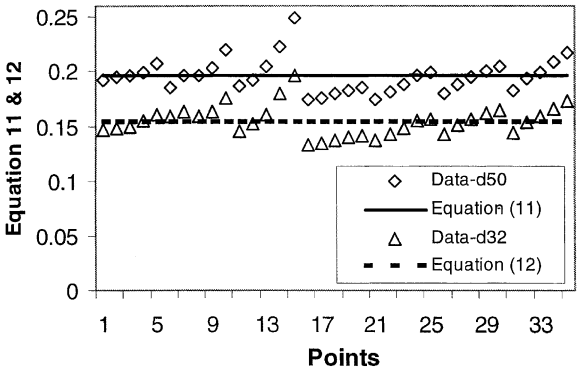


Fig. 14. Comparison data with Eqs. (11) and (12).

$$\left(\frac{d_{50}U_{SG}^2\rho_G}{\sigma}\right)^{0.37}\left(\frac{d_{50}}{D}\right)^{0.36}=0.196 \tag{11}$$

$$\left(\frac{d_{32}U_{SG}^2\rho_G}{\sigma}\right)^{0.55}\left(\frac{d_{32}}{D}\right)^{0.36}=0.154 \tag{12}$$

Eq. (11) is compared with measurements in the 2.54 cm pipeline and below centerline of the 9.53 cm pipeline in Fig. 14.

## 4. Discussion

The principal finding of this research is that the drop size increases with increasing pipe diameter and that $d_{50} \sim D^{0.5}$ at $U_{SG} > 30$ m/s.

An exact determination of the effect is complicated because the influence of liquid flow is not defined. The presently used method is to assume that drop size increases linearly with the volume

fraction of the core flow occupied by drops. This seems to imply that drop size increases by coalescence of drops. However, there is no direct evidence to support this explanation, nor has the assumption of a linear dependence at all values of the entrainment been verified. (There also could be an effect of liquid flow that is associated with the formation of drops.) Fortunately, the influence of liquid flow is smaller than the influence of gas velocity in annular flows, so that it can be ignored in a first approximation. Then Eqs. (11) and (12) can be used.

A log-normal distribution appears to fit the volume distribution function over a large range of drop sizes. This function requires the definition of a volume median diameter and a standard deviation. The later appears to be weakly dependent on gas velocity, liquid flow and pipe diameter, so that an approximate similarity is observed.

The log-normal distribution overpredicts the measurements at large and at small diameters. However, these deviations could be due, in part, to measurement errors. Evaporation and the withdrawal of drops through the wall of the porous suck-off section could lead to an underestimation of the number of small drops. Deposition in the suck-off section could lead to an underestimation of the number of large diameter drops.

An inherent concern is that the angular deviation due to diffraction decreases with increasing drop size. Thus, there is a limitation on the size of drops that can be measured accurately with the Malvern instrument. The curve fitting algorithms could, therefore, lead to erroneous estimates at larger drop diameters. However, the volume median diameters that are measured appear to be within the range that has been specified for the lens.

The results shown in Figs. 4–6 suggest the existence of a limiting drop size. Therefore, the use of an upper limit log-normal function has been a popular approach to predict the number of large diameter drops. Simmons and Hanratty (2001) explored this approach extensively. They used three parameters, a standard deviation, a median drop diameter, $d_{50}$, and a maximum drop diameter, $d_{max}$. These were selected so as to obtain a best fit to the data. A difficulty is that the $d_{max}$ obtained in this way appears to be too large.

Figs. 15 and 16 compares the use of log-normal and upper-limit log-normal distributions to fit measurements in the 2.54 cm pipe at $U_{SG} = 36$ m/s and $U_{SL} = 0.083$ m/s. In one of these (Fig. 15), $d_{max}$ is selected from a consideration of data shown in Figs. 4–6. In the other (Fig. 16), $d_{max}$ is treated as an empirical constant. Comparisons such as this indicate that it is not advantageous to use an upper limit distribution to represent measurements obtained in a 2.54 cm pipe.

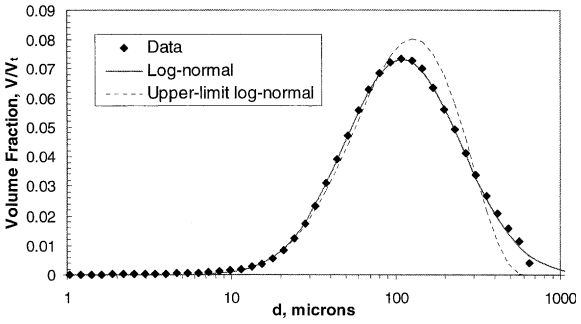


Fig. 15. Comparison of distribution functions fitting with measured data at $U_{SL} = 0.083$ and $U_{SG} = 36$ m/s ($d_{max}$ in the upper-limit log-normal = 653 μm, $\sigma = 0.78$, $d_{50} = 112$ μm).

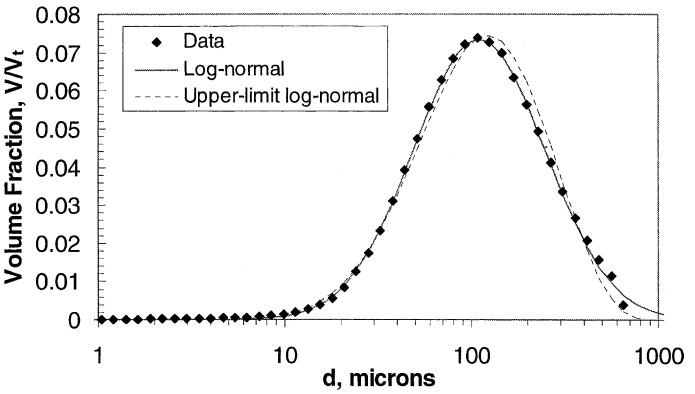


Fig. 16. Comparison of distribution functions fitting with measured data at $U_{SL} = 0.083$ and $U_{SG} = 36$ m/s ($d_{max}$ in the upper-limit log-normal is treated as an empirical constant = 1000 μm, $\sigma = 0.78$, $d_{50} = 112$ μm).

## Acknowledgements

This work was supported by the Engineering Program of the Division basic energy sciences at the department of energy under grant DOE DEF GO2-86ER-13556. The invaluable advice of engineers at Malvern is gratefully acknowledged.

## References

Al-Sarkhi, A., Hanratty, T.J., 2001. Effect of pipe diameter on the performance of drag-reducing polymers in annular gas–liquid flows. IchemE, Chem. Eng. Res. Design 79, 402–408.

Azzopardi, B.J., 1983. Mechanisms of entrainment in annular two-phase flow. AERE-R 11068.

Azzopardi, B.J., 1985. Drops sizes in annular two-phase flow. Exp. Fluids 3, 53–59.

Azzopardi, B.J., 1997. Drops in annular two-phase flow. Int. J. Multiphase Flow 23, 1–53.

Azzopardi, B.J., Zaidi, S.H., Sudlow, C.A., 1996. The effect of inclination on drop sizes in annular gas–liquid flow. European Two-Phase Flow group Meeting, Grenoble, 2–5 June 1996.

Dallman, J.C., 1978. Investigation of separated flow model in annular gas-liquid two phase flows. Ph.D. thesis, University of Illinois at Urbana-Champaign.

Hay, K.C., Liu, Z.C., Hanratty, T.J., 1996. Relation of deposition rate to drop size when the rate law is non-linear. Int. J. Multiphase Flow 22, 829–848.

Pan, L., Hanratty, T.J., 2002. A correlation of entrainment for annular flow in a horizontal pipe. Int. J. Multiphase Flow 28, 385–408.

Ribeiro, A.M., Bott, T.R., Jepson, D.M., 1995. Drop size and entrainment measurements in horizontal flow. In: Celata, G.P., Shah, R.K. (Eds.), Int. Conf. on Two-phase Flow Modeling and Experiment, Rome, 9–11 October, vol. 2. Pub Edizione ETS, Pisa, pp. 665–674.

Simmons, M., Hanratty, T.J., 2001. Droplet size measurements in horizontal annular gas–liquid flow. Int. J. Multiphase Flow 27, 861–883.

Tatterson, D.F., Dallman, J.C., Hanratty, T.J., 1977. Drop sizes in annular gas–liquid flows. AIChE J. 23, 68–76.

Williams, L.R., 1990. Effect of pipe diameter on horizontal annular two-phase flow. Ph.D. thesis, University of Illinois, Urbana.